



Removal of Thymol Blue from Aqueous Solution by Natural and Modified Bentonite: Comparative Analysis of ANN and ANFIS Models for the Prediction of Removal Percentage

Hülya Koyuncu^{1*}, Adnan Aldemir², Ali Rıza Kul³ and Murat Canayaz⁴

1. Department of Chemical Engineering, Faculty of Engineering and Natural Sciences, University of Bursa Technical, P.O.Box 16310, Bursa, Turkey
2. Department of Chemical Engineering, Faculty of Engineering, University of Van Yüzüncü Yıl, P.O.Box 65080, Van, Turkey
3. Department of Chemistry, Faculty of Science, University of Van Yüzüncü Yıl, P.O.Box 65080, Van, Turkey
4. Department of Computer Engineering, Faculty of Engineering, University of Van Yüzüncü Yıl, P.O.Box 65080, Van, Turkey

Received: 13 June 2021, Revised: 24 August 2021, Accepted: 18 September 2021

ABSTRACT

In this study natural bentonite (NB) and acid-thermal co-modified bentonite (MB) were utilized as adsorbents for the removal of Thymol Blue (TB) from aqueous solution. The batch adsorption experiments were conducted under different experimental conditions. The artificial neural network (ANN) and adaptive neuro fuzzy inference systems (ANFIS) were applied to estimate removal percentage (%) of TB. Mean squared error (MSE), root mean square error (RMSE) and coefficient of determination (R^2) values were used to evaluate the results. In addition, the experimental data were fitted isotherm models (Langmuir, Freundlich and Temkin) and kinetic models (pseudo first order (PFO), pseudo second order (PSO) and intra-particle diffusion (IPD)). The adsorption of TB on both the NB and MB followed well the PSO kinetic model, and was best suited Langmuir isotherm model. When the temperature was increased from 298 K to 323 K for 20 mg/L of TB initial concentration, the removal percentage of TB onto the NB and MB increased from 74.91% to 84.07% and 81.19% to 93.12%, respectively. This results were confirmed by the positive ΔH° values indicated that the removal process was endothermic for both the NB and MB. The maximum adsorption capacity was found as 48.7805 mg/g and 117.6471 mg/g for the NB and MB, respectively (at 323 K). As a result, with high surface area and adsorption capacity, the MB is a great candidate for TB dye removal from wastewater, and the ANFIS model is better than the ANN model at estimating the removal percentage of the dye.

Keywords: Adsorption, Bentonite, Thymol Blue, Artificial Neural Networks, ANFIS.

INTRODUCTION

Thymol Blue (TB) is known acid–base indicator in analytical chemistry. It is also used as a dye in some industries such as paint, leather and textile. The release of even very small amount of TB dye from the process wastewater to the environment can be caused harmful effects on human as well as animal life. Therefore, the removal of TB from effluents is very important. Although there are some methods such as adsorption, chemical coagulation, chemical oxidation, electrochemical treatment used to remove pollutants from wastewater,

* Corresponding Author Email: hulya.koyuncu@btu.edu.tr

adsorption is an important and most popular method among them due to high efficiency, low cost, simple application and availability (Du et al., 2017; Cheng et al., 2015; Ngulube et al., 2017 & Kausar et al., 2018).

Clays are known to have adsorption capacity for dyes, and their capacities are comparable with activated carbon which is the most popular adsorbent (Adeyemo et al., 2017). Recent studies conducted about the adsorption of dyes using clays have shown that some natural clays, bentonite in particular, demonstrate significant dye removal capacities, while others still require certain modifications to enhance their adsorption capacity (Leodopoulos et al., 2012). Bentonite which is negatively charged has three-layer silicate structure and due to having a great number of cations in its layers has high adsorption performance, and has attracted the attention of researchers as an adsorbent due to its low cost and high efficiency (Miyoshi et al., 2018; Kul & Koyuncu 2010; Oussalah et al., 2019 & Alexander et al., 2019).

The modelling of a process is conducted to obtain data about how that process will behave without carrying out experiments. Modelling is an accepted application for many processes in the fields of both science and engineering. Computational models are more flexible than statistical models when dataset including nonlinearities or insufficient (Ghaedi & Vafaei 2017). Artificial intelligence methods, such as artificial neural network (ANN) and adaptive neuro fuzzy inference systems (ANFIS), can be used to model adsorption (Ghaedi et al., 2015 & Banerjee et al., 2015). ANN based on biological nerve processing can be used to resolve and model a large number of complex engineering systems thanks to its simplicity, robustness, reliability and nonlinearity. There are some applications of ANN modeling in the literature (Poznyak et al., 2019). ANFIS, which is a very efficient tool similar to ANN, can be used for input and output relationships for describe nonlinear complicated systems. The ANFIS model is formed of the antecedent part and the conclusion part which emerged as a combination of fuzzy logic and ANN approaches, and is an effective tool that can be used to simulate nonlinear variations in complex systems (Dolatabadi et al., 2018). It is considered to be a technology with applications for the prediction of the performance of many processes owing to its universal ability to simulate nonlinear variations, and for extrapolation based on historical data in numerous fields. However, there are few studies conducted on the application of ANN and ANFIS for adsorption process.

The novelty of this study is the comparison of the adsorption performance of the natural bentonite (NB) and acid-thermal co-modified bentonite (MB) for Thymol Blue dye removal from aqueous media for the first time, and the investigation of the performance of the artificial neural network (ANN) and adaptive neuro fuzzy inference system (ANFIS) models with three statistical metrics.

The aim of this study was comparison of the adsorption performance of NB and MB for TB dye removal from aqueous media in terms of isotherm, kinetic and thermodynamic examinations. Also, this study aimed to predict the adsorption behaviour of NB and MB using ANN and ANFIS models. Since adsorption is a complex process and due to the complicated relationships between input and output parameters, it is a process that is difficult to model using statistical models. For the adsorption of TB on to NB and MB, initial concentration of TB, interaction time and temperature were considered the input data and the percentage of TB removal was calculated as the output data, using ANN and ANFIS.

MATERIALS & METHODS

The adsorption experiments were carried out with NB and MB clays. The NB sample was obtained from the province of Kütahya, Turkey. The XRF results of NB was observed as

follows: 71.60 wt.% SiO₂, 2.79 wt.% MgO, 13.15 wt.% Al₂O₃, 0.36 wt.% K₂O, 2.23 wt.% CaO, 0.66 wt.% Fe₂O₃, 0.26 wt.%, Na₂O, 0.07 wt.% TiO₂ and 8.45 wt.% loss of ignition. The NB was activated to increase its surface area and to change its physicochemical properties. For acid activation, a reactor made of pyrex glass, with a condenser, was used. Then 250 ml of 5N HCl solution was slowly added to 50 g of bentonite that had been placed in the reactor and allowed to stand for 3 hours under continuous stirring at a boiling temperature of around 105 °C. The bentonite samples were filtered and washed with distilled water in order to eliminate acid residues. Then, the solution was centrifuged at 4500 rpm for 5 minutes. After the final wash, the sample was centrifuged and incubated at 60 °C for 48 hours. Due to lumps forming during drying, the bentonite sample was milled. For thermal activation, the bentonite sample was heated to 600 °C for 24 hours and then stored in a desiccator after passing through 235 mesh sieves. Details of the NB and MB adsorbent preparation and characterization results were given in our previous study (Kul & Koyuncu 2010).

The chemical formula of TB is C₂₇H₃₀O₅S (molecular weight: 466.59 g/mol), while its IUPAC name is 4-[9-(4-hydroxy-2-methyl-5-propan-2-yl-phenyl)-7,7-dioxo-8-oxa-7λ6-thiabicyclo[4.3.0]nona-1,3,5-trien-9-yl]-5-ethyl-2-propan-2-yl-phenol. TB (CAS 76-61-9, 1081760025) was obtained from Merck (Germany) and other solvents with reagents were used without further purification. The stock solution of TB was prepared by dissolving a weighed quantity of TB in ethanol (95 percent). The required initial concentration of TB solutions (10, 20, 30, 40, 50, 60, 70 mg/L) used for the adsorption processes were prepared from the stock solution by diluting with double-distilled water.

In batch experiments, which were carried out in a temperature-controlled water bath (Julabo, EC-13A) 1 g bentonite was treated with 1L of TB solution, and the mixture was shaken at 300 rpm using shaker. All experiments were performed at pH 9.5 because of the highest removal (%) was taken at this pH value which was adjusted using 0.1 M HCl and 0.1 M NaOH solutions with a pH meter (Selecta, pH-2005). The TB concentration in the solution was determined for 140 min. The suspension was centrifuged (Nüve, NF800) at 5000 rpm for 10 min and then supernatant were analyzed for TB concentration by spectrophotometer (PG Instruments Ltd, T80/T80+) at 594 nm maximum absorbance wavelength. A calibration curve was prepared by plotting between the absorbance and various TB concentrations. The unknown TB concentrations were measured using the calibration curve. The same processes were carried out for NB and MB clays at 298 K, 308 K and 323 K temperatures. Each adsorption experiment was conducted in triplicate and average of the obtained data was taken as result. The adsorption capacity of TB by the adsorbent at equilibrium, q_e (mg/g) was determined with Eq. (1):

$$q_e = \frac{(C_0 - C_e) * V}{m} \quad (1)$$

where V is solution volume (L), C_0 is initial concentration of TB (mg/L) and C_e is equilibrium concentration of TB (mg/L), m is the clay mass (g). The TB removal percentage was determined with Eq. (2):

$$\text{Removal Efficiency (\%)} = \frac{(C_0 - C_e)}{C_0} * 100 \quad (2)$$

The effects of the initial TB concentration, temperature and contact time on removal of TB with NB and MB clays were investigated with two neural network modeling. The effect of

initial TB concentration was studied by initial concentration of TB dye solutions (10, 20, 30, 40, 50, 60, 70 mg/L).

Development of the Neural Networks:

ANN is an artificial intelligence application that analyses data and discovers new information from certain algorithms (Pauletto et al., 2020; Tayebi et al., 2019; Tajmiri et al., 2020 & Mahmodi-Balaban et al., 2019). The input data is multiplied by weight values and transmitted between neurons according to the values of the activation functions. These processes are repeated until the output is updated by training the weights and biases values with the input values. The purpose of the training is to find the weights and biases values that will produce the correct outputs for the examples shown to the network. In this way, the network reaches the correct weights and biases values and gains the ability to make generalizations about the event represented by the samples. The process of the network acquiring this generalization feature is called “learning the network”. The ANN structure developed in this study consisted of three layers. The first layer was a three-input layer (independent variables) which were contact time, initial concentration and temperature. The application was run by increasing the number of neurons from 3 to 10 in the hidden layer. The removal percentage of dye was obtained in the output layer (dependent variable). Input and output data were normalized in the range of 0-1. The following equation was used for normalization:

$$y = (x_i - x_{min}) / (x_{max} - x_{min}) \quad (3)$$

where y , x_{max} and x_{min} is the normalized, maximum and minimum values of x_i , respectively. The ANN structure for TB adsorption on NB or MB is given in Figure 1-a.

In the ANN structure, 85% of the data was used in the training process and 15% was used in the test process. The percentage of dye adsorption in solution was estimated by ANN structure. The Neural Network Toolbox in the MATLAB software was used for this application. Levenberg-Marquardt algorithm was used for optimization during ANN training. The tangent sigmoid function which is given in Eq. (4) was applied to the hidden layers.

$$f(x) = \frac{2}{(1 + \exp(-2x))} - 1 \quad (4)$$

The machine running the application had an I7 processor and 16 GB RAM. Mean squared error (MSE), root mean square error ($RMSE$) and coefficient of determination (R^2) values were used to evaluate performance which formulae used in calculation of these are given in the following equations, respectively.

$$MSE = \frac{1}{N} \sum_{i=1}^N (|y_{prd,i} - y_{exp,i}|)^2 \quad (5)$$

$$RMSE = \sqrt{\frac{\sum_{i=1}^N (y_{prd,i} - y_{exp,i})^2}{N}} \quad (6)$$

$$R^2 = 1 - \frac{\sum_{i=1}^N (y_{prd,i} - y_{exp,i})^2}{\sum_{i=1}^N (y_{prd,i} - y_m)^2} \quad (7)$$

where $y_{prd,i}$ is i_{th} predicted value, $y_{exp,i}$ is i_{th} observed value, y_m is mean value of $y_{exp,i}$, and N is number of observations in the experimental studies. R^2 showed that predicted output variable estimation curve fitted experimental output variable curve.

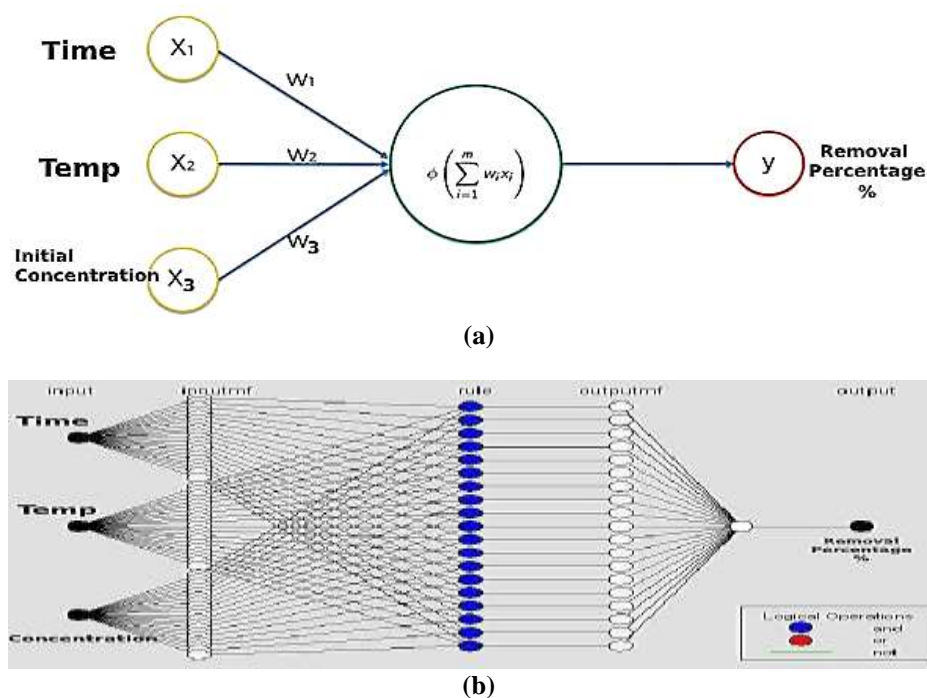


Figure 1. ANN model (a) and ANFIS model (b) structures for TB adsorption on the NB and MB.

ANFIS has a wide application area as a special network structure that integrates the learning ability of ANNs with the inference ability of fuzzy systems (Shankar et al., 2018 & Canayaz 2019). As the if-then rule structure uses input and output values, it is often used in forecasting problems that require decision-making mechanisms. An ANFIS learning algorithm is a mixed learning algorithm consisting of the combined use of least squares method and backpropagation learning algorithm. There are two steps in the hybrid learning algorithm: forward transition and backward transition. In the forward transition process, the resultant parameters are fixed while they are updated using least squares estimates. In the backward transition process, result parameters are fixed and back propagation gradient descent method is used to update precursor parameters. Forward and backward transitions are repeated with a certain number of iterations and training is completed. ANFIS consists of five layers: fuzzification, rule, normalization, defuzzification and output. ANFIS tries to obtain an inference by generalizing the input samples to the output with these layers. In this structure, rules are created for the values that are taken as input. In the application used in this study there were three inputs and removal percentage was obtained as output value. In the ANFIS structure, due to lack of validation process, the data were divided into two sets: training (80%) and test (20%). The data were also mixed before starting the training. The ANFIS structure for TB adsorption on NB and MB is given in Figure 1-b.

Many isotherm models are used to identify the adsorption of dyes on solid surfaces. For the interaction between adsorbate molecules and adsorbent surface, the well-established Langmuir, Freundlich and Temkin models were chosen in this study. Three models were applicable for descriptions of the experimental results obtained at three different temperatures for NB and MB. The parameters of three isotherm model equations were calculated by regression using the linear form of their equations (Ghaleh et al., 2020).

There are assumptions about adsorption occurrence on a homogenous surface and no interaction between adsorbates in the plane of surface in Langmuir isotherm model which equation is given with Eq. (8):

$$q_e = (q_m K_L C_e) / (1 + K_L C_e) \quad (8)$$

where q_m denotes the maximum capacity of adsorption (mg/g), C_e represents equilibrium concentration of solution (mg/L), K_L is a Langmuir constant associated with affinity of the binding sites and energy of adsorption (L/g). A linear form of Eq. (8) was obtained when $1/C_e$ versus $1/q_e$ was plotted, and q_m and K_L can be determined from the slope and intercept.

Freundlich isotherm is an empirical model based on adsorption on a heterogeneous surface and this isotherm equation is given with Eq. (9):

$$q_e = K_F C_e^{1/n} \quad (9)$$

where K_F is Freundlich constant linked to adsorption capacity of adsorbate (L/g), and $1/n$ is an empirical parameter connected to adsorption intensity with $n > 1$ represents favorable adsorption conditions. A linear form of Eq. (9) was obtained when the logarithm of q_e versus C_e was plotted. The line slope and intercept show n and K_F values respectively.

Temkin isotherm model considers effect of the adsorbate interaction on adsorption, which is given with Eq. (10):

$$q_e = B \ln(K_T C_e) \quad (10)$$

where K_T is equilibrium binding constant and B is related to adsorption heat which is given with Eq. (11):

$$B = RT/b_T \quad (11)$$

where $1/b_T$ indicates the removal potential of adsorbent, R is the gas constant, T is the temperature (K). B and K_T values for different temperatures.

Kinetic models were applied to check experimental results of TB adsorption onto the NB and MB. The adsorption kinetic is important to choose the best test circumstances for the adsorption process with the batch technique. The kinetic parameters for estimation of adsorption rate provide vital knowledge for designing and modelling adsorption processes. Kinetic models are widely used in adsorption operations to investigate the mechanisms that control the removal process, such as the adsorption surface, chemical reaction and/or diffusion mechanisms (Cheruiyot et al., 2019). In this study, TB adsorption kinetics were calculated using pseudo first order (PFO), pseudo second order (PSO) and intra-particle diffusion (IPD) kinetic models. The best fit model was chosen depending on the correlation coefficient (R^2) values. These models were investigated according to experimental data at various temperatures and initial TB concentrations.

Lagergren's kinetics equation can be used first for the characterization of adsorption systems depending on solid capacity. Lagergren's equation, which is named the pseudo first order (PFO) kinetic model, separates the equation depending on concentration of solution and solid adsorption capacity (Lagergren & Svenska 1898). The PFO linear model is given Eq. (12):

$$\ln(q_e - q_t) = \ln q_e - k_1 t \quad (12)$$

where k_1 (1/min) is rate constant of PFO model. To achieve constants of this model, plots of $\ln(q_e - q_t)$ against t are drawn.

Pseudo second order kinetic model which explains chemical bond formation between adsorbent and adsorbate molecules based on adsorption capacity (Ho & McKay 1998). The linear form of PSO model based on adsorption capacity is given with Eq. (13):

$$\frac{t}{q_t} = \frac{1}{(k_2 q_e^2)} + \frac{t}{q_e} \quad (13)$$

where k_2 represents rate of adsorption (g/mg.min), values of k_2 and q_e were identified from intercept and slope of plot of t/q_t versus t according to Eq. (13).

Activation energy of this removal process is calculated from the Arrhenius equation is given with Eq. (14):

$$\ln k_2 = \ln k_0 - \frac{E_A}{RT} \quad (14)$$

where k_2 is rate constant (g/mol.s), k_0 is temperature independent factor (g/mol.s), E_A is activation energy (J/mol), R is gas constant (8.314 J/mol.K) and T is adsorption temperature (K).

Adsorption of dyes was more gradual when intra-particle diffusion (IPD) was the rate controlling step. According to Weber & Morris (1963), IPD model assumes that the chemical or physical bond formed between solute and solid in interspatial sites on the solid control the overall speed of the adsorption. The possibility of intra-particle diffusion as the rate limiting step was tested using the IPD model, which can be represented by an Eq. (15):

$$q_t = k_{ipd} t^{0.5} + C \quad (15)$$

where k_{ipd} (mg/g min^{0.5}) is IPD rate constant and C is boundary thickness which are determined with plot of q_t against $t^{0.5}$ at different TB concentrations.

Thermodynamic investigation is required to determine the importance of adsorption process. The changes of Gibbs free energy ΔG° (kJ/mol), enthalpy ΔH° (kJ/mol), and entropy ΔS° (kJ/mol.K) are significant to detect heat alterations during the adsorption process. The thermodynamic parameters of TB adsorption onto NB and MB adsorbents were calculated by the equations given below:

$$\Delta G^\circ = -RT \ln K_d \quad (16)$$

$$\Delta G^\circ = \Delta H^\circ - T \Delta S^\circ \quad (17)$$

$$\ln K_d = \frac{\Delta S^\circ}{R} - \frac{\Delta H^\circ}{RT} \quad (18)$$

where K_d is equilibrium constant (q_e/C_e ; L/g). R is gas constant and T is temperature (K). ΔH° and ΔS° parameters are calculated from slope and intercept of plot of $\ln K_d$ versus $1/T$.

RESULTS AND DISCUSSION

Nitrogen adsorption isotherms of the NB and MB were given in Figure 2-a, and the Brauner-Emmett-Teller (BET) surface areas of the samples were also determined. The acid activation caused formation of smaller pores in solid particles resulting higher surface area (109.80

m^2/g) relative to than NB ($71.95 \text{ m}^2/\text{g}$). The samples had almost mesopores of which diameters were between $20\text{-}500 \text{ \AA}$. The NB and MB samples exhibited maxima in differential pore volumes at about 39.46 \AA and 34.50 \AA in pore diameter respectively (Figure 2-b). The cation exchange capacities (CEC) of the NB and MB were found as 65 and $97 \text{ meq}/100 \text{ g}$, respectively (Kul & Koyuncu 2010).

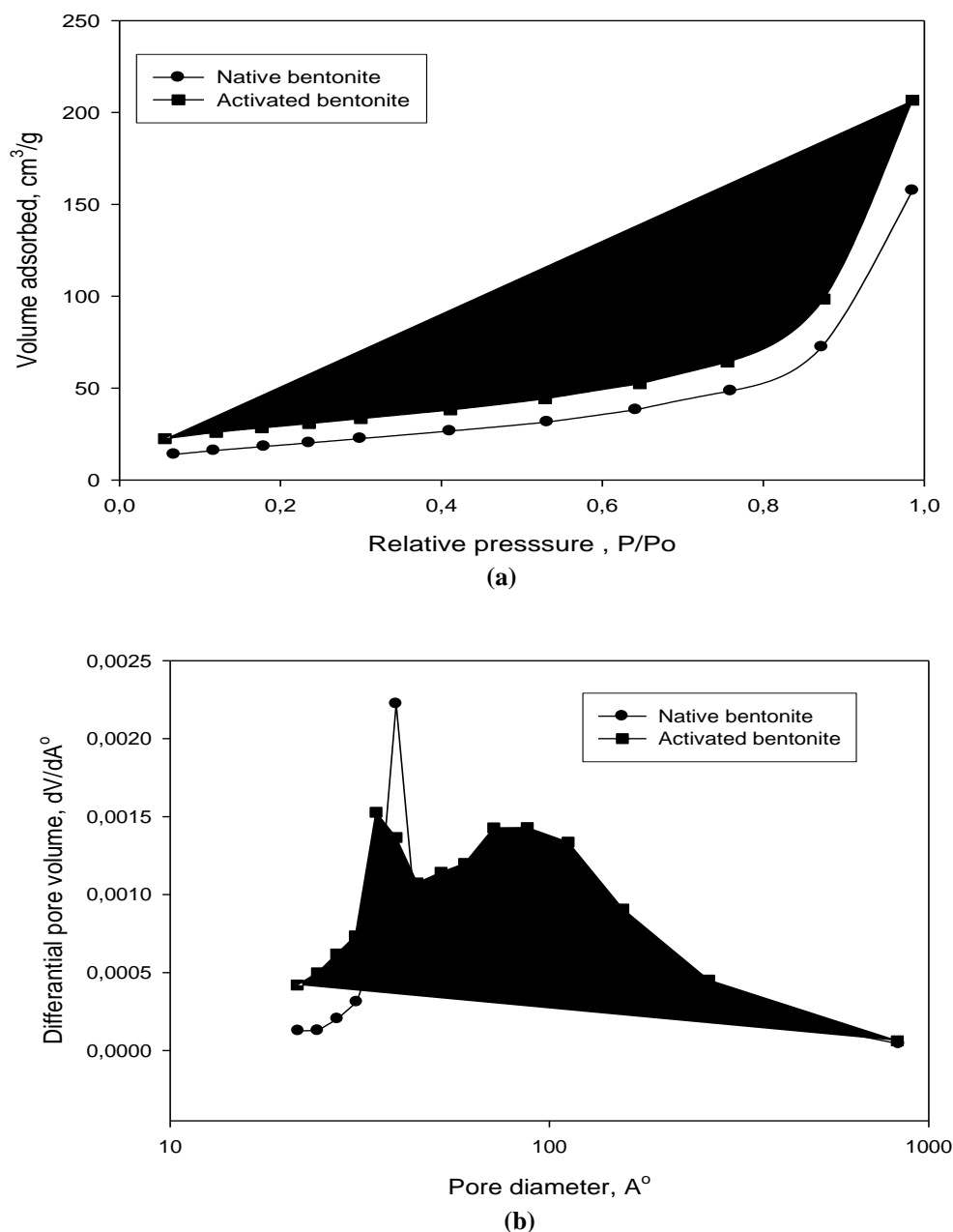
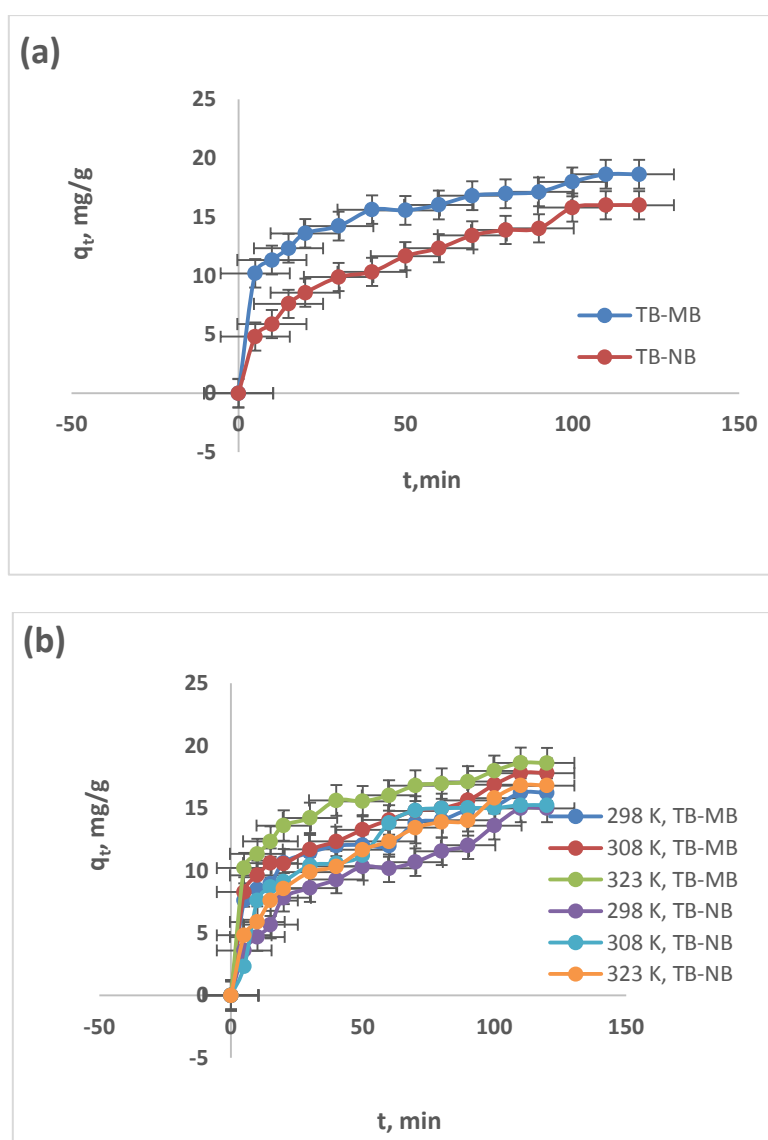


Figure 2. Nitrogen adsorption isotherms (a) and pore size distributions (b) of the NB and MB.

In the adsorption experiments, firstly, studies were carried out to determine the most appropriate pH and adsorbent dose for the highest adsorption performance. The optimum pH and adsorbent dosage values were determined as 9.5 and $1 \text{ g}/\text{L}$, respectively (Figures were not given). The effect of interaction time on the adsorption of TB onto the NB and MB was studied to determine equilibrium time. As shown in Figure 3-a, the fast adsorption of TB

occurred within the first 30 min and the equilibrium was set up after 110 min for both NB and MB. The effect of temperature on the adsorption of TB on NB and MB was investigated and the results shown in Figure 3-b. The adsorption capacity increased with increase in temperature because the mobility of TB molecules increased with increase in their kinetics. Also, it can be explained that the endothermic adsorption enthalpy. In addition, the adsorption capacity increased with increasing initial TB concentration, while the removal efficiency (%) of TB decreased with increasing initial TB concentration for both NB and MB (Figure 3-c). The removal efficiencies (%) of TB onto NB were found as 74.91%, 76.17% and 84.07% at 298 K, 308 K and 323 K, respectively (20 mg/L initial concentration of TB), while the removal percentages for MB were determined as 81.19%, 89.06% and 93.12% at 298 K, 308 K and 323 K, respectively (20 mg/L initial concentration of TB). Besides, it was found that the removal efficiency (%) of TB with the MB was higher than NB in all studied solution concentration and temperatures.



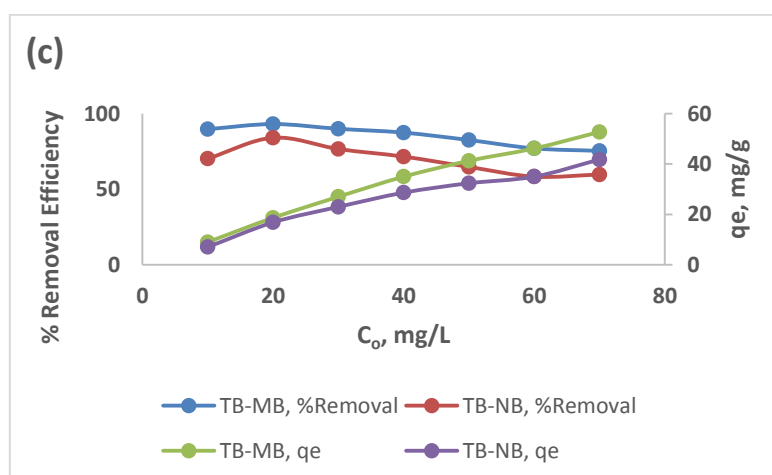


Figure 3. Effect of various parameters on the adsorption performance ((a): interaction time effect (C_0 : 20 mg/L, 323 K), (b): temperature effect (C_0 : 20 mg/L, 323 K) and (c): initial TB concentration effect on adsorption capacity and removal (%) (323 K)).

The performance results obtained from the ANN model for NB and MB adsorbents were given in Table 1. According to results with training of network, R^2 values for 10 neurons were determined as 0.9732 and 0.9887 for NB and MB adsorbents, respectively. The performance results of obtained from NB and MB were compared and it was seen that the R^2 values of MB adsorbent were higher than the R^2 values of NB adsorbent. The MSE and the $RMSE$ values were also very low and it was seen that the MSE and the $RMSE$ values of MB adsorbent were lower than that of the NB adsorbent. This is an important parameter indicating that ANN had high generalization capability. Figure 4-(a and c) shows the regression plots and the MSE values obtained by ANN model for NB. It can be seen from the performance results in Figure 4-(a and c) that the ANN reached the best value with a low epoch number. R^2 values for TB adsorption onto NB adsorbent were obtained as 0.98 for training, validation, test and all data.

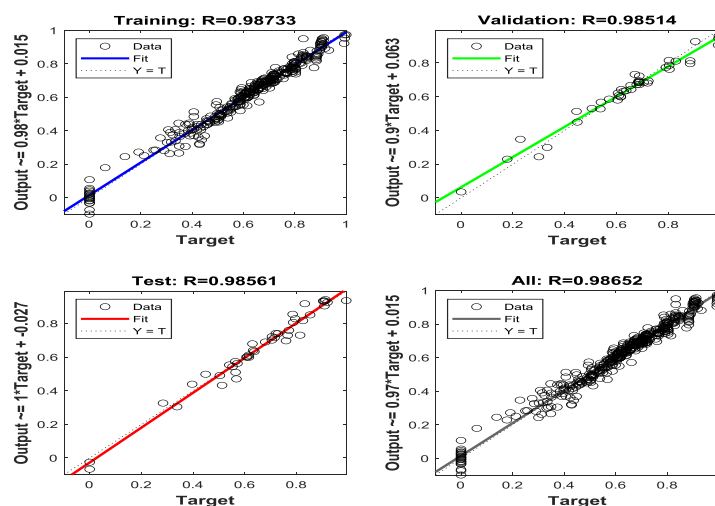
Table 1. Comparison of performance values for TB adsorption onto NB and MB using ANN model

Number of Neurons	NB			MB		
	R^2	$RMSE$	MSE	R^2	$RMSE$	MSE
3	0.9381	0.0536	0.0029	0.9605	0.0436	0.0019
5	0.9469	0.0497	0.0025	0.9819	0.0295	0.0009
7	0.9658	0.0399	0.0016	0.9867	0.0252	0.0006
9	0.9701	0.0373	0.0014	0.9872	0.0248	0.0006
10	0.9732	0.0353	0.0012	0.9887	0.0233	0.0005

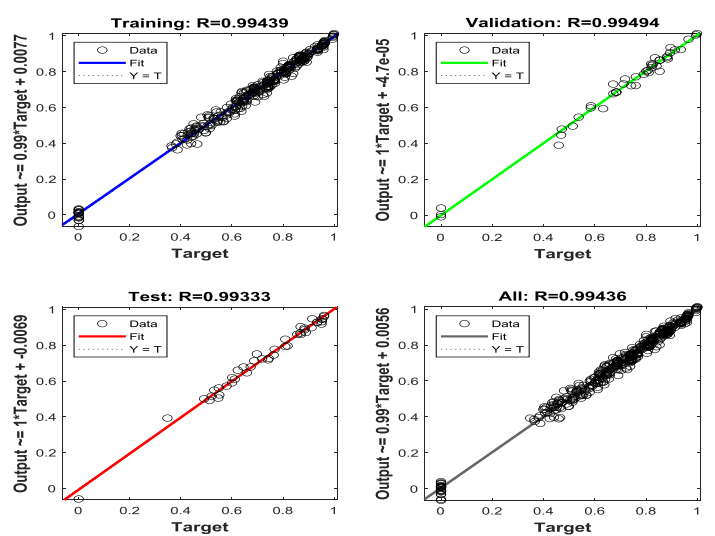
The obtained regression and performance plots by using the ANN model for MB are given in Figure 4-(b and d). According to the regression plots of TB adsorption onto MB adsorbent, R^2 values were obtained as 0.99 at the applied conditions. The MSE against number of epochs for ANN shows that method performance does not change after 40 epochs. As shown in the performance graphs, the best values were obtained with lower epoch numbers compared to the results of NB. ANN model applications for dye adsorption under various conditions were reviewed in the literature (Ghaedi & Vafaei 2017). The obtained values in this study and those obtained in the literature indicate that the ANN model showed good performance.

The grid partitioning (genfis1), subtractive clustering (genfis2) and fuzzy c-means (genfis3) structures were used for this study. The results of ANFIS analysis were obtained by

using genfis1, genfis2 and genfis3 tools in MATLAB. The parameter values used for genfis1 were as follows: number of MFs: 5, inputmf: gaussmf and outputmf: linear. The parameter values used for genfis2 were as follows: influence radius: 0.3, maximum number of epochs: 75, fis type: sugeno, inputmf: gaussmf and outputmf: linear. The parameter values used for genfis3 were as follows: number of clusters: 15, partition matrix exponent: 2, maximum number of iterations: 200, minimum improvement: $1e-5$. The obtained MSE, RMSE and R^2 values were given in Table 2 for training and test data for TB adsorption onto NB and MB adsorbents. In addition, Figure 5 shows the training and test data for the ANFIS results of TB adsorption onto NB and MB adsorbents, respectively. Based on the ANFIS results, it can be seen that in Table 2 the highest R^2 values were obtained as 0.9985 with genfis2 and 0.9483 with genfis3 for MB and NB, respectively. In addition, it was seen that MSE and $RMSE$ results are low and MSE , $RMSE$ and STD values for genfis1 and genfis2 were lower than genfis3 for NB and MB. When these results are compared with the ANN results, it is clear that ANFIS produced better results. Due to the error between the experimental and predicted outputs, it was determined that ANFIS provided high accuracy and efficiency for the prediction of TB adsorption.



(a)



(b)

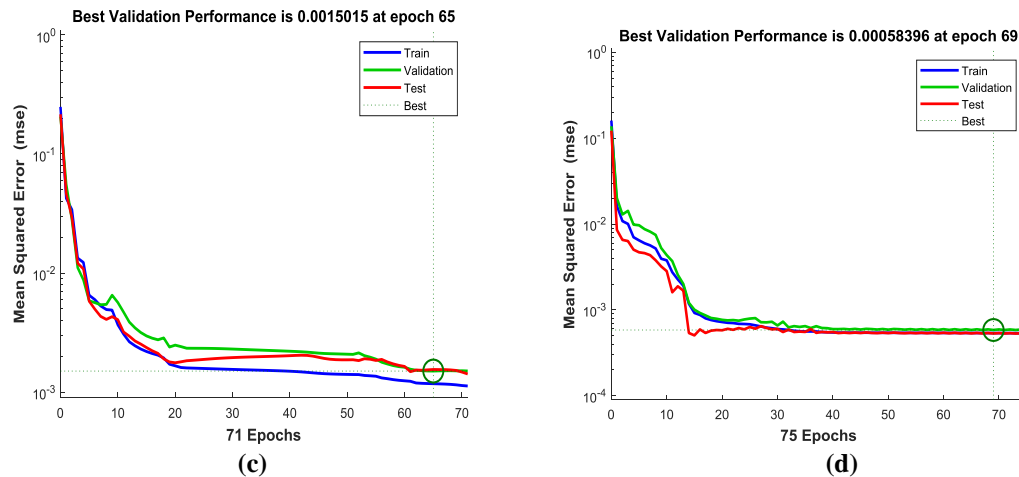
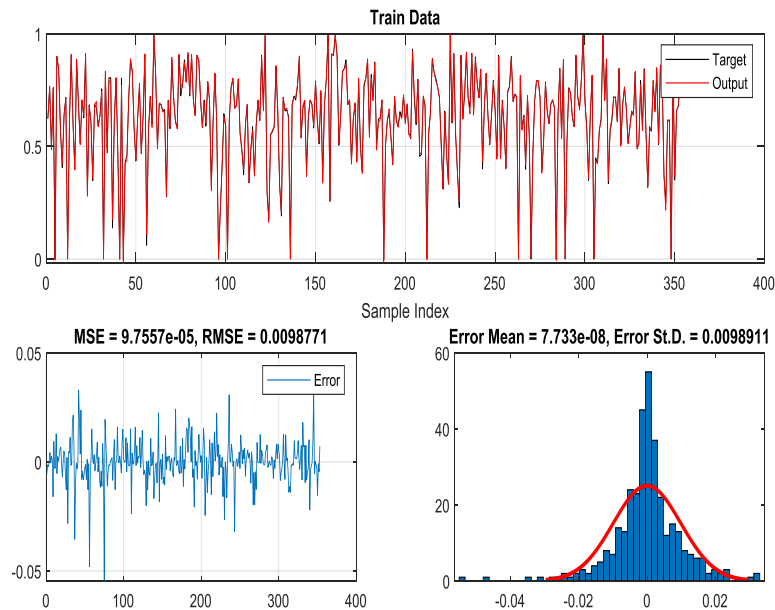


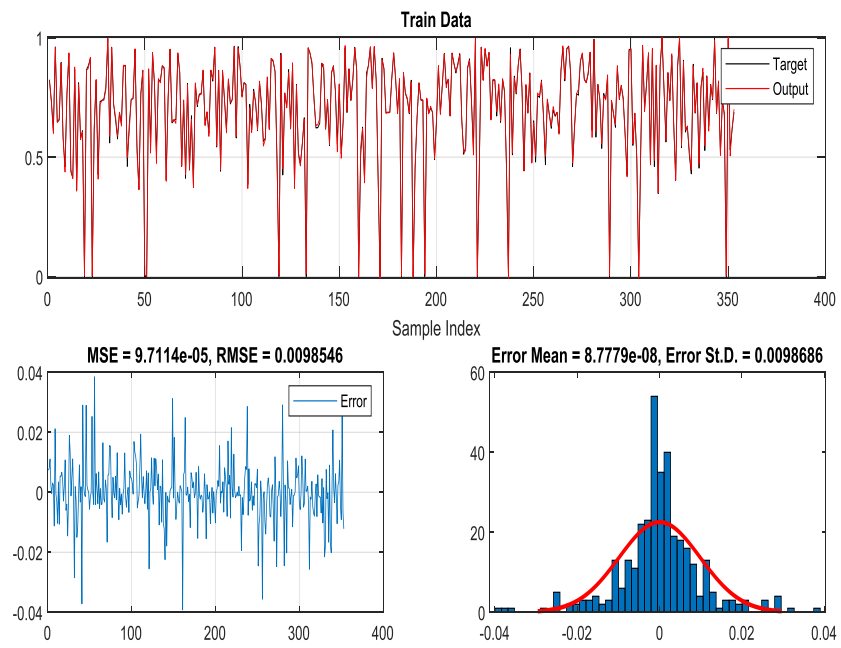
Figure 4. ANN plots for TB adsorption; the regression results for NB (a) and MB (b), and the performance results for NB (c) and MB (d).

In this study, it was used the methods like a train/test split only to estimate the ability of the model to generalize to new data. Too little learning and the model will perform poorly on the training dataset and on new data. The model will underfit the problem. Too much learning and the model will perform well on the training dataset and poorly on new data, the model will overfit the problem. In both cases, the model has not generalized. Three models can be considered: Underfit model; A model that fails to sufficiently learn the problem and performs poorly on a training dataset and does not perform well on a holdout sample. Overfit model; A model that learns the training dataset too well, performing well on the training dataset but does not perform well on a hold out sample. Good fit model; A model that suitably learns the training dataset and generalizes well to the hold out dataset.

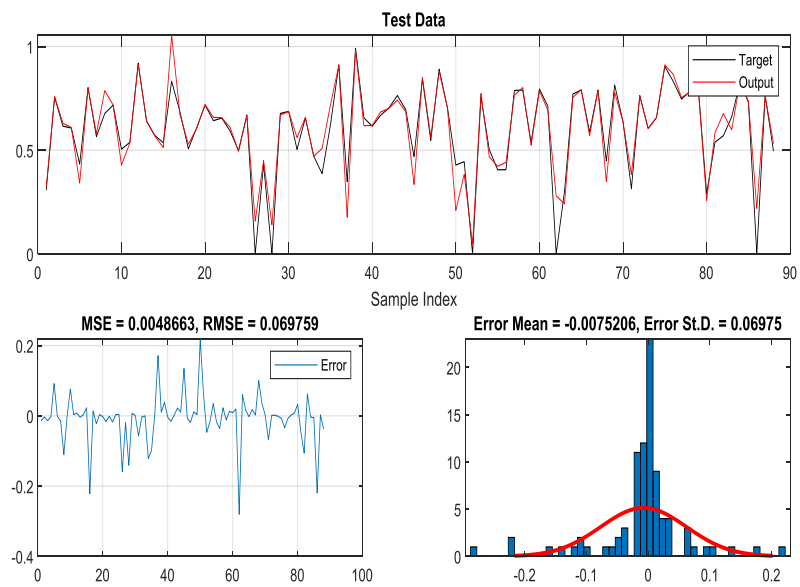
From the Figure 5-b, it is possible to see that the model works properly for train, test, and validation data. In addition, it can be stated that it is a good fit model, not over-fitting (Figure 5).



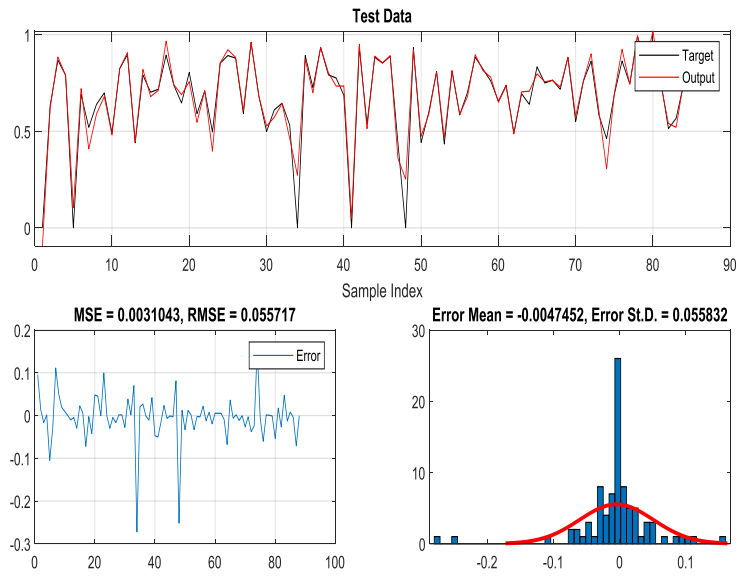
(a)



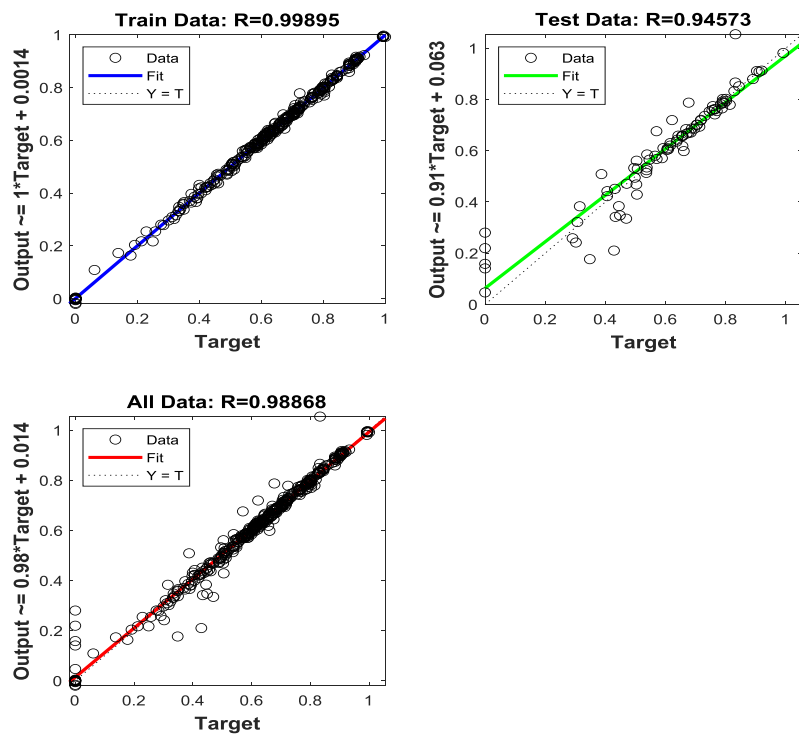
(b)



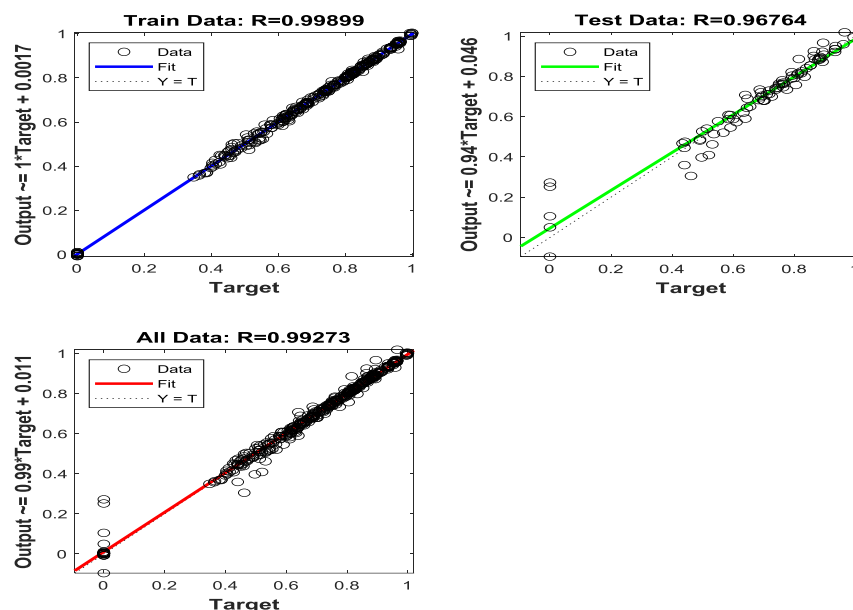
(c)



(d)



(e)



(f)

Figure 5. ANFIS plots for TB adsorption; training data results of genfis2 for NB (a) and MB (b), test data results of genfis2 for NB (c) and MB (d), regression plots of genfis2 for NB (e) and MB (f).

The efficiencies of ANN and ANFIS models were verified by evaluating their performances using statistical metrics. The *MSE* and *RMSE* values of ANN results for TB adsorption onto NB and MB adsorbents were obtained as 0.00192, 0.00093 and 0.04316, 0.02928, respectively. In addition, R^2 values greater than 0.95 and 0.98 were found for NB and MB adsorbents, respectively. These results indicate sufficient adjustment among experimental and predicted values by ANN. These values were determined to be within acceptable range (Ghosal et al., 2018; Madan et al., 2016; Yıldız & Uzun 2015 & Mondal et al., 2017). The *MSE* and *RMSE* values of ANFIS results for TB adsorption onto NB and MB adsorbents were determined 0.00019, 0.00021 and 0.04312, 0.04611, respectively. These values were found to be within range reported in the literature. The R^2 values were close to 1.00 compared to those found by the ANN and ANFIS models (Ghaedi et al., 2014; Baghban et al., 2017 & Rego et al., 2018).

Table 2. Comparison of performance values for TB adsorption onto NB and MB using ANFIS model

ANFIS models		Training				Test			
		<i>MSE</i>	<i>RMSE</i>	R^2	<i>STD</i>	<i>MSE</i>	<i>RMSE</i>	R^2	<i>STD</i>
genfis1	NB	0.0002	0.0133	0.9962	0.0134	0.0142	0.1193	0.6615	0.1163
	MB	0.0001	0.0102	0.9979	0.0102	0.0077	0.0879	0.8206	0.0874
genfis2	NB	0.0001	0.0099	0.9979	0.0099	0.0049	0.0698	0.8932	0.0697
	MB	0.0001	0.0099	0.9985	0.0099	0.0031	0.0557	0.9358	0.0558
genfis3	NB	0.0009	0.0294	0.9824	0.0295	0.0019	0.0431	0.9483	0.0433
	MB	0.0011	0.0314	0.9804	0.0314	0.0021	0.0463	0.9461	0.0459

Langmuir, Freundlich and Temkin isotherms were plotted for NB and MB adsorbents at different temperatures (Figures not given), and the results of these models were given in Table 3.

R^2 values for the three isotherms were relatively high for both NB and MB. The Langmuir isotherm results obtained from NB and MB adsorbents were compared and it was seen that the R^2 values of MB were higher than that of NB for all studied concentration and temperatures. Besides, the obtained constants of three isotherms (K_L , K_F , K_T) and the determined q_m values of MB were higher than that of NB for TB adsorption (Table 3). In the Langmuir isotherm, q_m represents the maximum adsorption of TB with monolayer capacity. The maximum adsorption capacity was found as 48.7805 mg/g and 117.6471 mg/g for NB and MB, respectively (at 323 K). It can be stated that the maximum adsorption capacity found in this study is relatively higher than that of the reported many studies. q_m values for the removal of TB from aqueous solution were determined as 50 mg/g and 5.28 mg/g by using multi-wall carbon nanotube and pomegranate peel, respectively (Hamad & Hanan 2018; Raoufi & Aghaie 2017). The separation factor R_L ($1/(1 + K_L C_0)$) which indicates the adsorption was favourable or not was calculated at various temperatures and given in Table 3. Values of R_L obtained for both NB and MB were between 0 and 1 which supported the applicability of Langmuir model. In the Freundlich model, when the temperature was raised from 298 K to 323 K, K_F values increased which supported endothermic nature of the adsorption, and $1/n$ values decreased which confirmed the favorably adsorption of TB onto NB and MB. The plots of Temkin isotherm have positive slopes for NB and MB adsorbents which are implies a repulsive lateral interaction exists in the adsorption layer (Cheng et al., 2015). The values of B which was related to the heat of adsorption obtained using Temkin isotherm model increased with increasing temperature and supported higher adsorption capacity (Table 3). B values were calculated as 13.0970 J/mol and 14.0490 J/mol for NB and MB, respectively (323 K).

Table 3. Isotherm parameters of TB adsorption onto NB and MB

	Temp (K)	Langmuir				Freundlich			Temkin		
		K_L (L/g)	q_m (mg/g)	R_L	R^2	K_F (L/g)	$1/n$	R^2	K_T (L/g)	B (J/mol)	R^2
NB	298	0.1105	40.9836	0.3116	0.9617	6.6933	0.4747	0.9435	0.5302	12.1090	0.9478
	308	0.1424	43.8596	0.2599	0.9123	8.2334	0.4524	0.9529	0.6381	12.7990	0.9688
	323	0.1252	48.7805	0.2853	0.9570	10.7984	0.3875	0.9809	0.6782	13.0970	0.9611
MB	298	0.0474	97.0874	0.5131	0.9655	6.7924	0.6124	0.9100	1.0494	13.1720	0.9654
	308	0.0539	108.6957	0.4808	0.9476	8.3469	0.6037	0.8705	1.4745	13.5480	0.9650
	323	0.0824	117.6471	0.3775	0.9893	12.6999	0.5329	0.8940	2.2470	14.0490	0.9850

The PFO, PSO and IPD model plots were shown in Figure 6 for NB and MB adsorbents, and the results of parameters were given in Table 4. Experimental and calculated q_e values for MB were higher than that of NB, and the calculated q_e values at 323 K were higher than that of 298 K and 308 K for both NB and MB. R^2 coefficients were higher than 0.98 with experimental and calculated q_e values very close to each other indicating that this adsorption process well fit the PSO than the PFO and IPD kinetic models for both NB and MB (Figure 6-(a and b)). Polyethyleneimine modified bentonite and natural bentonite and/or cetyl trimethyl ammonium bromide modified bentonite were used for some dye removal, and similar results were found (Huang et al., 2017 & Du et al., 2017). In addition, kinetic data obtained from dye adsorption processes by using various adsorbents were better fit PSO model than other kinetic models due to the higher values of R^2 (Yagub et al., 2014).

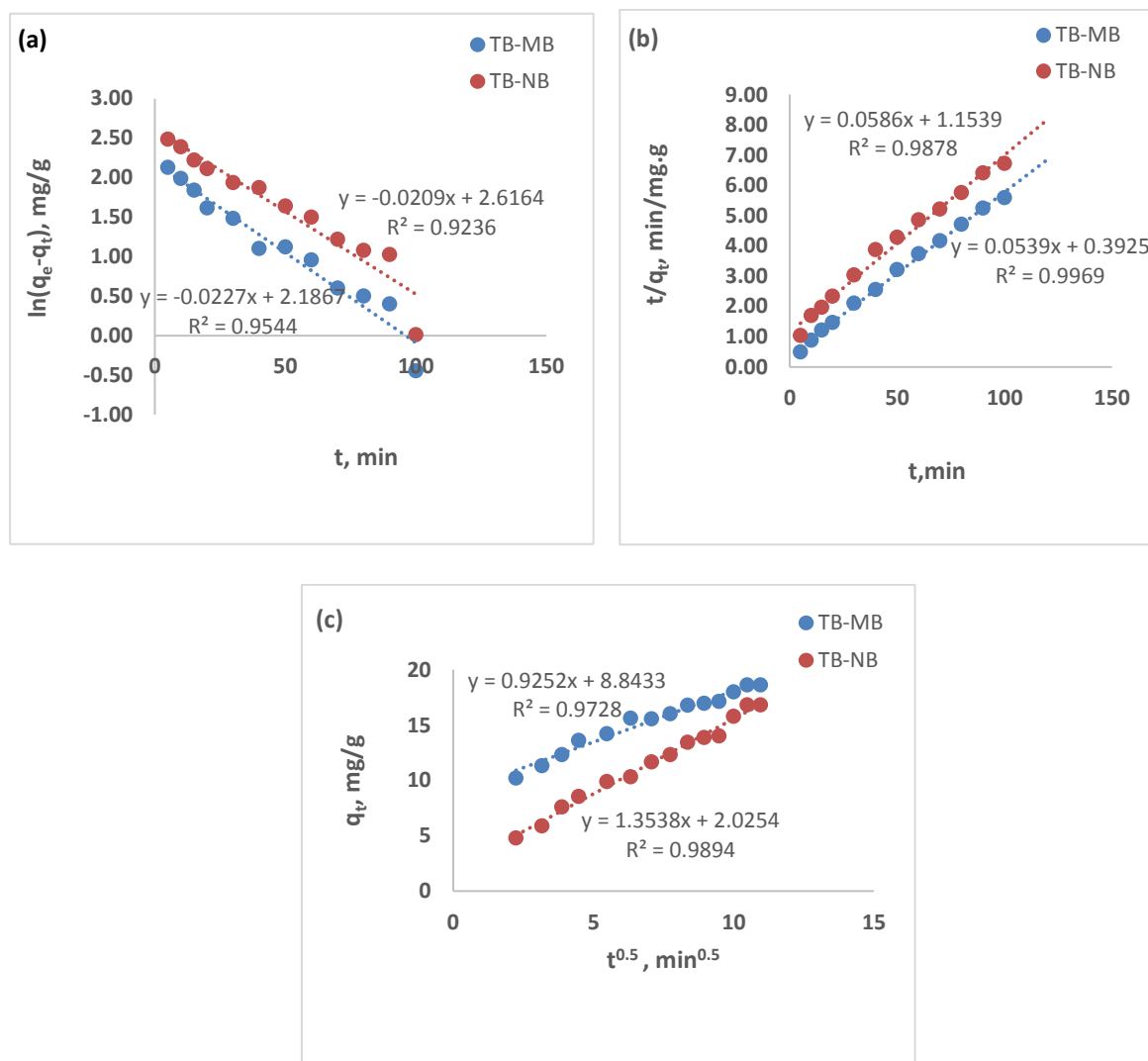


Figure 6. PFO (a), PSO (b) and IPD (c) plots for the adsorption of TB onto the NB and MB ($C_0 = 20$ mg/L, 323 K).

In the IPD model, a relatively high R^2 values were obtained for both NB and MB. This indicated that the model can be used to describe the mechanism of adsorption kinetics. The IPD plots (Figure 6-c) were linear and did not pass through the origin. This deviation from the origin can be owing to the changing of the mass transfer rate in the initial and final process of the adsorption. This was explained that the transfer of TB molecules has occurred some steps such as external diffusion from the aqueous phase to the surface of the adsorbents, internal diffusion on the NB and MB surfaces, intra-particle pore diffusion and adsorption on the pore surfaces.

The intra-particle diffusion of TB molecules into the pores of the adsorbents was a slow process, and intra-particle pore diffusion was involved in the adsorption of TB onto both the NB and MB (Koyuncu & Kul 2020). Therefore, it can be stated that the intra-particle diffusion included in the adsorption process but was not only a rate controlling step.

Table 4. The PFO, PSO and IPD kinetic parameters of TB adsorption onto the MB and NB (equilibrium time 110 min, $C_o = 20$ mg/L)

Kinetic model	Temp (K)	Kinetic parameter	MB	NB	
PFO	298	$q_{e \text{ exp}}$ (mg/g)	16.237	14.981	
	308	$q_{e \text{ exp}}$ (mg/g)	17.811	15.233	
	323	$q_{e \text{ exp}}$ (mg/g)	18.624	16.813	
	298	k_1 (min^{-1})	0.0197	0.0175	
		$q_{e \text{ cal}}$ (mg/g)	10.9496	11.8924	
		R^2	0.9208	0.9153	
	308	k_1 (min^{-1})	0.0201	0.0462	
		$q_{e \text{ cal}}$ (mg/g)	9.7299	13.6864	
		R^2	0.9443	0.9236	
	323	k_1 (min^{-1})	0.0227	0.0209	
		$q_{e \text{ cal}}$ (mg/g)	8.9058	17.0713	
		R^2	0.9544	0.9248	
PSO	298	k_2 (g/mg.min)	0.00430	0.00219	
		$q_{e \text{ cal}}$ (mg/g)	16.0772	15.1057	
		R^2	0.9829	0.9756	
	308	k_2 (g/mg.min)	0.00489	0.00271	
		$q_{e \text{ cal}}$ (mg/g)	17.5131	15.6739	
		R^2	0.9841	0.9618	
	323	k_2 (g/mg.min)	0.00740	0.00298	
		$q_{e \text{ cal}}$ (mg/g)	18.5528	17.0649	
		R^2	0.9969	0.9878	
	IPD	298	k_{id} (mg/g.min ^{0.5})	0.9727	1.2292
			C	5.5443	1.1993
			R^2	0.9728	0.9678
308		k_{id} (mg/g.min ^{0.5})	1.0653	1.2854	
		C	5.9486	2.6694	
		R^2	0.9866	0.8930	
323	k_{id} (mg/g.min ^{0.5})	0.9252	1.3538		
	C (mg/g)	8.8433	2.0254		
	R^2	0.9728	0.9894		

The validity of the kinetic models (PFO, PSO and IPD) was determined by calculating the RMSE and the deviation (%) between the experimental and calculated q_e values (Table 5).

It was found a good agreement between the experimental and the calculated q_e values for the PSO model. The deviations (%) were found as 0.3823 and 1.4983 for the MB and NB, respectively. These values were lower than that of the PFO and IPD kinetic models (Table 5). So, it can be stated that the adsorption of TB onto both the MB and NB follows well the PSO kinetics. In addition, the smaller RMSE values for the PSO and IPD models were shown that the IPD model was also involved in the explanation of the adsorption mechanism for both the NB and MB.

Table 5. The model validity evaluation ($C_o = 20$ mg/L, 323 K)

	PFO	PSO	IPD
<u>MB</u>			
RMSE	9.5762	0.5899	0.2538
Deviation (%)	34.7616	0.3823	0.4145
<u>NB</u>			
RMSE	7.8481	0.9753	0.4190
Deviation (%)	40.7006	1.4983	3.5026

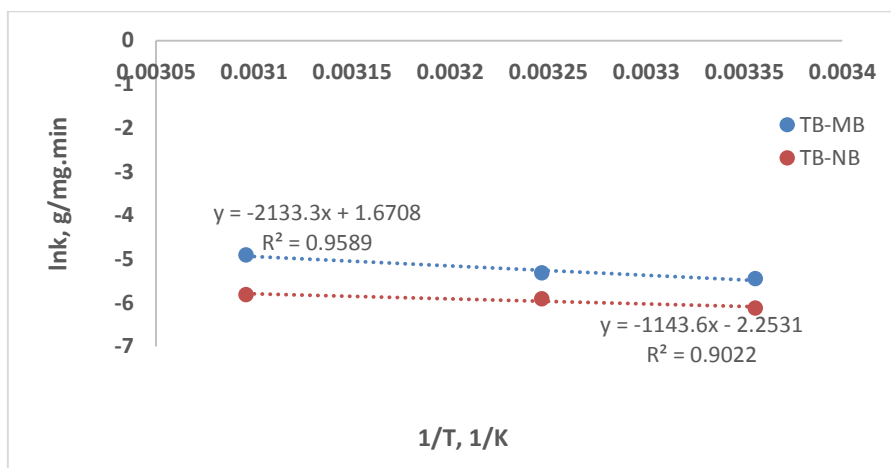


Figure 7. The Arrhenius plots for NB and MB.

From the Arrhenius plots (Figure 7), the values of the activation energy (E_A) of TB adsorption onto NB and MB adsorbents were calculated as 9.5079 kJ/mol and 17.7363 kJ/mol, respectively.

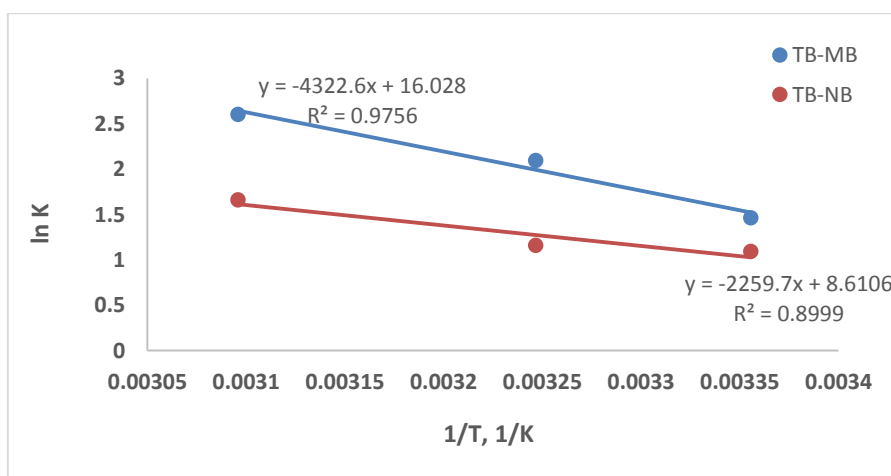


Figure 8. Van't Hoff plots for the adsorption of TB onto NB and MB.

Thermodynamic parameters assist in describing the mechanism of the adsorption process. The change of Gibbs free energy ΔG° (kJ/mol) was calculated from Eq.(16). The slope and intercept of Van't Hoff plots (Figure 8) gave ΔH° (kJ/mol) and ΔS° (kJ/mol.K), respectively. The calculated thermodynamic parameters for TB adsorption onto NB and MB were summarized in Table 6.

Table 6. Thermodynamic parameters of TB adsorption onto NB and MB

Adsorbent	Temp (K)	ΔG° (kJ/mol)	ΔH° (kJ/mol)	ΔS° (kJ/mol.K)	R^2
NB	298	-2.7087	18.7872	0.0716	0.8999
	308	-2.9728			
	323	-4.4630			
MB	298	-3.6248	35.9381	0.1332	0.9756
	308	-5.3669			

The ΔG° values were calculated to be in the range of -2.7087 – -4.4630 kJ/mol for NB and -3.6248 – -6.9878 kJ/mol for MB. The ΔG° values decreased with rising temperatures which indicated that this separation process was better at higher temperatures. Besides, the negative values of the ΔG° showed feasibility and spontaneous nature of the adsorption for both NB and MB. The ΔH° and ΔS° values were determined as 18.7872 kJ/mol and 0.0716 kJ/mol.K for NB and 35.9381 kJ/mol and 0.1332J/mol.K for MB, respectively. The positive ΔH° value indicated that the removal process was endothermic for both NB and MB. It was also confirmed by increasing q_e values with rising temperatures. The positive ΔS° values implied enhanced randomness at the TB-NB and TB-MB interface and affinity of the NB and MB for TB (Souza et al., 2019).

CONCLUSION

The adsorption of TB onto the NB and MB adsorbents were investigated under different experimental conditions. The ANN and ANFIS models were successfully applied to estimate the removal percentage of TB. Due to the error between the experimental and predicted outputs, it was determined that ANFIS provided high accuracy and efficiency for the prediction of TB adsorption. Kinetic studies indicated that the adsorption of TB onto both the NB and MB was best described by the PSO model and also fitted the IPD. Isotherm studies showed that the Langmuir and Temkin models were best suited to the experimental data. It was found that the maximum adsorption capacity and the removal percentage of TB on the MB were higher than that of the NB. Thermodynamic parameters demonstrated that this removal process was endothermic, feasible and spontaneous for both the NB and MB.

As a result, it can be stated that the MB can be used as a promising adsorbent for remediation of wastewater, and the ANFIS model can be applied to estimate the removal percentage of dyes from aqueous media.

GRANT SUPPORT DETAILS

The present research did not receive any financial support.

CONFLICT OF INTEREST

The authors declare that there is not any conflict of interests regarding the publication of this manuscript. In addition, the ethical issues, including plagiarism, informed consent, misconduct, data fabrication and/ or falsification, double publication and/or submission, and redundancy has been completely observed by the authors.

LIFE SCIENCE REPORTING

No life science threat was practiced in this research.

REFERENCES

- Adeyemo, A.A., Adeoye I.O. and Bello, O.S. (2017). Adsorption of dyes using different types of clay: a review. *Appl. Water. Sci.* 7, 543–568.
- Alexander, J.A., Zaini, M.A.A., Surajudeen, A., Aliyu, E.N.U. and Omeiza, A.U. (2019). Surface modification of low-cost bentonite adsorbents - a review. *Part. Sci. Technol.* 37(5), 538-549.

- Baghban, A., Bahadori, A., Mohammadi, A.H. and Behbahaninia, A. (2017). Prediction of CO₂ loading capacities of aqueous solutions of absorbents using different computational schemes. *Int. J. Greenh. Gas Con.* 57, 143–161.
- Banerjee, P., Sau, S., Das, P. and Mukhopadhyay, A. (2015). Optimization and modelling of synthetic azo dye wastewater treatment using graphene oxide nanoplatelets: characterization toxicity evaluation and optimization using artificial neural network. *Ecotoxicol. Environ. Saf.* 119, 47–57.
- Canayaz, M. (2019). Training anfis system with moth-flame optimization algorithm. *Int. J. Intell. Syst. Appl. Eng.* 7(3), 133-144.
- Cheng, Y., Feng, Q., Ren, X., Yin, M., Zhou, Y. and Xue, Z. (2015). Adsorption and removal of sulfonic dyes from aqueous solution onto a coordination polymeric xerogel with amino groups. *Colloids Surf. A.* 485, 125-135.
- Cheruiyot, G.K., Wanyonyi, W.C., Kiplimo, J.J. and Maina, E.N. (2019). Adsorption of toxic crystal violet dye using coffee husks: Equilibrium, kinetics and thermodynamics study. *Scientific African.* 5, 00116.
- Dolatabadi, M., Mehrabpour, M., Esfandyari, M., Alidadi, H. and Davoudi, M. (2018). Modeling of simultaneous adsorption of dye and metal ion by sawdust from aqueous solution using of ANN and ANFIS. *Chemometr. Intell. Lab. Syst.* 181, 72-78.
- Du, S., Wang, L., Xue, N., Pei, M., Sui, W. and Guo, W. (2017). Polyethyleneimine modified bentonite for the adsorption of amino black 10B. *J. Solid. State Chem.* 252, 152-157.
- Ghaedi, A.M. and Vafaei, A. (2017). Applications of artificial neural networks for adsorption removal of dyes from aqueous solution: a review. *Adv. Colloid Interface Sci.* 245, 20-39.
- Ghaedi, M., Daneshfar, A., Ahmadi, A. and Momeni, M.S. (2015). Artificial neural network-genetic algorithm based optimization for the adsorption of phenol red (PR) onto gold and titanium dioxide nanoparticles loaded on activated carbon. *J. Ind. Eng. Chem.* 21, 587-598.
- Ghaedi, M., Hosaininia, R., Ghaedi, A.M., Vafaei, A. and Taghizadeh, F. (2014). Adaptive neurofuzzy inference system model for adsorption of 1,3,4-thiadiazole-2,5-dithiol onto gold nanoparticles-activated carbon. *Spectrochim. Acta A.* 131. 606–614.
- Ghaleh, S.P., Khodapanah, E. and Tabatabaei-Nezhad, S.A. (2020). Comprehensive monolayer two-parameter isotherm and kinetic studies of thiamine adsorption on clay minerals: experimental and modeling approaches. *J. Mol. Liq.* 306, 112942.
- Ghosal, P.S., Kattil, K.V., Yadav, M.K. and Gupta, A.K. (2018). Adsorptive removal of arsenic by novel iron/olivine composite: insights into preparation and adsorption process by response surface methodology and artificial neural network. *J. Environ. Manage.* 209, 176–187.
- Hamad, M.I.H. and Hanan, M.M.A. (2018). Removing of thymol blue from aqueous solutions by pomegranate peel. *The Third International Conference On Basic Sciences & Their Applications.* 1(1), 111-119.
- Ho, Y.S. and McKay, G. (1998). Kinetic models for the sorption of dye from aqueous solution by wood. *Process Saf. Environ. Prot.* 76(B2), 183-191.
- Huang, Z., Li, Y., Chen, W., Shi, J., Zhang, N., Wang, X., Li, Z., Gao, L. and Zhang, Y. (2017). Modified bentonite adsorption of organic pollutants of dye wastewater. *Mater. Chem. Phys.* 202, 266-276.
- Kausar, A., Iqbal, M., Javed, A., Aftab, K., Nazli, Z.H., Bhatti, H.N. and Nouren, S. (2018). Dyes adsorption using clay and modified clay: A review. *J. Mol. Liq.* 256, 395-407.
- Koyuncu, H. and Kul, A.R. (2020). Synthesis and characterization of a novel activated carbon using nonliving lichen *Cetraria islandica* (L.) ach. and its application in water remediation: Equilibrium, kinetic and thermodynamic studies of malachite green removal from aqueous media. *Surf. Interfaces.* 21, 100653.
- Kul, A.R. and Koyuncu, H. (2010). Adsorption of Pb(II) ions from aqueous solution by native and activated bentonite: kinetic equilibrium and thermodynamic study. *J. Hazard. Mater.* 179, 332-339.
- Langergren, S. and Svenska, B.K. (1898). Zur theorie der sogenannten adsorption gelöster stoffe *Veternskapsakad Handlingar.* 24, 1-39.

- Leodopoulos, Ch., Doulia, D., Gimouhopoulos, K. and Triantis, T.M. (2012). Single and simultaneous adsorption of methyl orange and humic acid onto bentonite. *Appl. Clay. Sci.* 70, 84-90.
- Madan, S.S., Wasewar, K.L. and Pandharipande, S.L. (2016.) Modeling the adsorption of benzene acetic acid on CaO₂ nanoparticles using artificial neural network. *Resour. Tech.* 2, 53–62.
- Mahmoodi-Babolan, N., Heydari, A. and Nematollahzadeh, A. (2019). Removal of methylene blue via bioinspired catecholamine/starch superadsorbent and the efficiency prediction by response surface methodology and artificial neural network-particle swarm optimization. *Bioresour. Technol.* 294, 1-8.
- Miyoshi, Y., Tsukimura, K., Morimoto, K., Suzuki, M. and Takagi, T. (2018). Comparison of methylene blue adsorption on bentonite measured using the spot and colorimetric methods. *Appl. Clay. Sci.* 151, 140-147.
- Mondal, S., Aikat, K., Siddharth, K., Sarkar, K., DasChaudhury, R., Mandal, G. and Halder, G. (2017). Optimizing ranitidine hydrochloride uptake of parthenium hysterophorus derived N-biochar through response surface methodology and artificial neural network. *Process Saf. Environ. Prot.* 107, 388–401.
- Ngulube, T., Gumbo, J.R., Masindi, V. and Maity, A. (2017). An update on synthetic dyes adsorption onto clay based minerals: a state-of-art review. *J. Environ. Manage.* 191, 35-57.
- Oussalah, A., Boukerroui, A., Aichour, A. and Djellouli, B. (2019). Cationic and anionic dyes removal by low-cost hybrid alginate/natural bentonite composite beads: adsorption and reusability studies. *Int. J. Biol. Macromol.* 124, 854-862.
- Pauletto, P.S., Gonçalves, J.O., Pinto, L.A.A., Dotto, G.L. and Salau, N.P.G. (2020). Single and competitive dye adsorption onto chitosan-based hybrid hydrogels using artificial neural network modeling. *J. Colloid Interface Sci.* 560, 722-729.
- Poznyak, A., Chairez, I. and Poznyak, T. (2019). A survey on artificial neural networks application for identification and control in environmental engineering: biological and chemical systems with uncertain models. *Annu. Rev. Control.* 48, 250-272.
- Raoufi, F. and Aghaie, H. (2017). Adsorption of thymol blue and Erythrosine-B on MWCNTs functionalized by N-(3-nitrobenzylidene)-N'-trimethoxysilylpropyl-ethane-1,2-diamine: equilibrium, kinetics and thermodynamic study. *Orient J. Chem.* 33(5), 2542-2550.
- Rego, A.S.C., Valim, I.C., Vieira, A.A.S., Vilani, C. and Santos, B.F. (2018). Optimization of sugarcane bagasse pretreatment using alkaline hydrogen peroxide through ANN and ANFIS modelling. *Bioresour. Technol.* 267, 634–641.
- Shankar, K., Elhoseny, M., Lakshmanaprabu, S.K., Ilayaraja, M., Vidhyavathi, R.M., Elsoud, M.A. and Alkhambashi, M. (2018). Optimal feature level fusion based ANFIS classifier for brain MRI image classification. *Concurrency Computat. Pract. Exper.* 32, 4887.
- Souza, P.R., Dotto, G.L. and Salau, N.P.G. (2019). Experimental and mathematical modeling of hindered diffusion effect of cationic dye in the adsorption onto bentonite. *J. Environ. Chem. Eng.* 7, 1-7.
- Tajmiri, S., Azimi, E., Hosseini, M.R. and Azimi, Y. (2020). Evolving multilayer perceptron, and factorial design for modelling and optimization of dye decomposition by bio-synthesized nano CdS-diatomite composite. *Environ. Res.* 182, 1-13.
- Tayebi, H.A., Ghanei, M., Aghajani, K. and Zohrevandi, M. (2019). Modeling of reactive orange 16 dye removal from aqueous media by mesoporous silica/crosslinked polymer hybrid using RBF MLP and GMDH neural network models. *J. Mol. Struct.* 1178, 514-523.
- Weber, W.J. and Morris, J.C. (1963). Kinetics of adsorption on carbon from solution. *J. Sanit. Eng. Div.* 89, 31-60.
- Yagub, M.T., Sen, T.K., Afroze, S. and Ang, H.M. (2014). Dye and its removal from aqueous solution by adsorption: a review. *Adv. Colloid Interface Sci.* 209, 172-184.
- Yıldız, Z. and Uzun, H. (2015). Prediction of gas storage capacities in metal organic frameworks using artificial neural network. *Micropor. Mesopor. Mat.* 208, 50–54.